HHS Public Access

Author manuscript

J Magn Reson Imaging. Author manuscript; available in PMC 2017 July 25.

Published in final edited form as:

J Magn Reson Imaging. 2015 October ; 42(4): 1039–1047. doi:10.1002/jmri.24863.

Differentiating Benign From Malignant Vertebral Fractures Using T_1-Weighted Dynamic Contrast-Enhanced MRI

Julio Arevalo-Perez, MD[1,*], **Kyung K. Peck, PhD**[1,2], **John K. Lyo, MD**[1], **Andrei I. Holodny, MD**[1], **Eric Lis, MD**[1], and **Sasan Karimi, MD**[1]

[1]Department of Radiology, Memorial Sloan-Kettering Cancer Center, New York, New York, USA

[2]Department of Medical Physics, Memorial Sloan-Kettering Cancer Center, New York, New York, USA

Abstract

Purpose—To differentiate pathologic from benign vertebral fractures, which can be challenging. We hypothesized that dynamic contrast-enhanced magnetic resonance imaging (DCE-MRI) can aid in the noninvasive distinction between pathologic and benign fractures.

Materials and Methods—Consecutive patients with vertebral fractures who underwent DCE-MRI, biopsy, and kyphoplasty were reviewed. Forty-seven fractures were separated into pathologic and benign fractures. Benign fractures were in turn separated into acute and chronic fractures for further comparison. Regions of interest (ROIs) were placed over fractured vertebral bodies. Perfusion parameters: plasma volume (V_p), K^{trans}, wash-in slope, peak enhancement, and area under the curve (AUC) were measured and compared between the three different groups of fractures. A Mann– Whitney *U*-test was conducted to assess the difference between the groups.

Results—Pathologic fractures had significantly higher ($P < 0.01$) perfusion parameters (V_p, K^{trans}, wash-in slope, peak enhancement, and AUC) compared with benign fractures. We also found significant differences ($P < 0.001$) in all parameters between chronic and acute fractures. V_p and K^{trans} were able to differentiate between pathologic and acute fractures ($P < 0.01$). No significant differences were found with peak enhancement ($P = 0.21$) and AUC ($P = 0.4$) between pathologic and acute fractures.

Conclusion—Our data demonstrate that T_1-weighted DCE-MRI has potential to differentiate between pathologic vs. benign, acute vs. chronic, and most important, benign acute vs. pathologic vertebral fractures.

Vertebral Compression Fractures in the thoracic or lumbar spine are a problem commonly encountered in daily clinical practice, particularly in elderly patients. Osteoporosis is the most common cause of compression fractures in this age group.[1] However, the spine is also a frequent location of metastatic and primary neoplastic disease that may result in pathologic fractures. Therefore, differentiation between malignant from benign fractures due to osteoporosis can be challenging, especially among cancer patients, who are prone to

[*]Address reprint requests to: J.A.-P., Department of Radiology, Memorial Sloan-Kettering Cancer Center, 1275 York Ave., New York, NY 10065. arevalj1@mskcc.org.

developing both types. Vertebral fractures are a very common concern in this cohort of patients who may be subject to long-term use of steroids, chemotherapy, radiotherapy, and frequently present with poor nutrition in addition to advanced age, factors that affect bone density.[2] Most metastatic tumors as well as primary neoplasms such as multiple myeloma are characterized by the presence of osteolytic lesions presenting with decreased bone density and osseous structural weakness. Besides certain treatment regimens, for instance, blocking sex hormones such as estrogen in breast cancer, can also affect bone mineral homeostasis.[2] All these circumstances put these patients at higher risk for vertebral fractures.

Magnetic resonance imaging (MRI) is a method for the detection and evaluation of bone-marrow pathologies to the point of becoming the imaging modality of choice for marrow metastatic disease.[3–6] Typically, for the standard clinical assessment, a qualitative analysis based on T_1- weighted spin-echo (SE) as well as short-T_1 inversion recovery (STIR) sequences is performed.[7] However, it is frequently difficult to distinguish between acute benign and pathologic compression fractures on conventional MRI since signal intensity changes are often similar.[8] Morphological features can be helpful, but can be misleading. For instance, pathological fractures due to multiple myeloma are notorious for mimicking osteoporotic fractures.[9] Marrow hypersignal on T_2-weighted images in neoplastic disorders is mainly due to intracellular water, whereas in acute fractures it reflects interstitial water (edema), thus complicating the characterization of fractures by using only conventional MRI.[10]

Recently, new contrast mechanisms allow a quantitative analysis of various aspects of bone physiology.[7] Particularly, dynamic contrast-enhanced (DCE) MRI perfusion imaging permits to obtain functional information on tumor vascularity and hemodynamics. A quantitative assessment of vascular features can be achieved by applying a pharmacokinetic model of contrast uptake to the calculated signal intensity changes over time. Considering a 2-compartment kinetic model, the contrast agent is presumed to be distributed in the blood plasma volume, leaking in a time-dependent manner into the interstitium.[11] This can provide quantitative estimation of perfusion parameters such as plasma volume (V_p) that represents the tumor vascularity or K^{trans} that represent the permeability constant of the vessel.[11,12] A number of studies have evaluated DCE-MRI in the characterization of musculoskeletal tumors and in the differentiation of benign from malignant masses. Some studies have shown that perfusion parameters can aid in the differentiation between normal bone marrow and malignant infiltration.[13–17]

The objective of this study was to assess, using a 2- compartment pharmacokinetic model analysis, the diagnostic value of DCE-MRI perfusion parameters as a noninvasive method to distinguish between pathologic and benign vertebral fractures.

Materials and Methods

Study Design

This retrospective study was granted a Waiver of Authorization by the Institutional Review Board. In compliance with the Health Insurance Portability and Accountability Act (HIPPA)

regulations and with approval of the hospital Privacy Board, we retrospectively reviewed patients with vertebral fractures from a data base of kyphoplasty procedures in our institution. The database was queried to select all patients with vertebral fractures who had undergone both biopsy and DCE-MRI perfusion studies between January 2012 and March 2014.

Patient Selection

Consecutive patients with vertebral fractures who underwent DCEMRI, biopsy, and kyphoplasty were reviewed. Forty-seven fractures were divided into pathologic and benign fractures. Patients without a preprocedure DCE perfusion scan between the above-mentioned dates were excluded. Studies with imaging artifact (osteosynthesis material, motion artifact, decreased signal-to-noise ratio) affecting the area of interest were also excluded. Histopathology reports were reviewed to determine the biopsy results of every fracture. The eligible remaining 21 patients (9 female, 12 male; 46–84 years old, mean age = 65 years old) presenting 47 fractures were included in the study. Acute and chronic fractures were present simultaneously in two patients. All fractures were divided into two groups depending on whether the results of the biopsy were pathologic (metastatic or primary tumor) or nonpathologic (without evidence of malignant cells) (Table 1).

Benign fractures were in turn divided into two subgroups, acute and chronic fractures, according to the presence of marrow edema on STIR sequences. We defined fractures from an imaging standpoint and considered a fracture acute as long as there was marrow edema, and chronic when there was no longer marrow edema. We did not define it in terms of days since sometimes the fractures were clinically occult (Table 2). The first group consisted of four patients (three female, one male: 55–70 years old, mean age = 62.5 years old) with 13 chronic osteoporotic fractures. The second group consisted of seven patients (three female, four male: 55–84 years old, mean age = 69.5 years old) with acute osteoporotic vertebral fractures. All individuals from the benign group had been diagnosed with concomitant neoplastic processes, although all biopsy results from the fractured vertebral bodies taken during the kyphoplasty procedure were negative for malignant cells. Patients in the chronic fracture group were diagnosed with ovarian adenocarcinoma ($n = 1$), glioblastoma ($n = 1$), multiple myeloma ($n = 1$), and sarcoma ($n = 1$). Patients in the acute fracture group included glioblastoma ($n = 4$), multiple myeloma ($n = 1$), esophageal adenocarcinoma ($n = 1$), and gallbladder adenocarcinoma ($n = 1$). The third group comprised 12 patients (four female, eight male: 46–77 years old, mean 61.5 years) with 19 pathologic fractures. The biopsy results were consistent with metastasis of a known primary neoplasm: lung adenocarcinoma ($n = 3$), colon adenocarcinoma ($n = 3$), gastric adenocarcinoma ($n = 2$), renal cell carcinoma ($n = 1$), prostate adenocarcinoma ($n = 1$), breast adenocarcinoma ($n = 1$), and melanoma ($n = 1$).

MRI Data Acquisition

MRI sequences of the spine were acquired with a 1.5T GE scanner (Milwaukee, WI) using an 8-channel cervical-thoracic-lumbar (CTL) surface coil. All patients underwent routine MRI, including sagittal T_1 (field-of-view [FOV], 32–36 cm; slice thickness, 3 mm; repetition time [TR], 400–650 msec; flip angle [FA], 90°) and T_2 (FOV, 32–36 cm; slice

thickness, 3 mm; TR, 3500–4000 msec; FA, 90°) and sagittal STIR (FOV, 32–36 cm; slice thickness, 3 mm; TR, 3500–6000 msec; FA, 90°).

DCE-MRI of the spine was then acquired. A bolus of gadolinium-diethylenetriamine pentaacetic acid (Gd-DTPA) was administered by a power injector at 0.1 mmol/kg body weight and a rate of 2 to 3 mL/sec. The kinetic enhancement of tissue during and after injection of Gd-DTPA was obtained using a 3D T_1-weighted fast spoiled-gradient (SPGR) echo sequence (TR, 4–5 milliseconds; echo time [TE], 1–2 milliseconds; slice thickness, 5 mm; FA, 25°; FOV, 32 cm; temporal resolution (Δt) of 6.5 seconds and consisted of 10–12 images in the sagittal plane. The 3D SPGR sequences generated phase images in addition to the standard magnitude images. The duration of the DCE sequence was 300 seconds. Sagittal and axial T_1-weighted post-Gd-DTPA MR images were acquired after DCE-MRI.

Data Analysis

Data processing and analysis was performed using dynamic image processing software (NordicIce-NeuroLab, Bergen, Norway) and MatLab (MathWorks, Natick, MA). Preprocessing steps included background noise removal, spatial and temporal smoothing, and detection of the arterial input function (AIF) from the aorta. AIF was individually calculated in each acquisition of every patient. Appropriate shape of the AIF curve was visually confirmed before processing steps continued. The Tofts 2-compartment pharmacokinetic model analysis was applied for calculation of voxel-by-voxel estimates of quantitative and semiquantitative perfusion parameters, including time-dependent leakage (K^{trans}), blood plasma volume (V_p) wash-in slope, peak enhancement, and area under the curve (AUC) maps.[11] All regions of interests (ROIs) were placed in the areas with high plasma flow in the fractured vertebral body on the perfusion maps by two radiologists (J.A.P. and S.K.) with 7 and 16 years of experience, respectively, who were blinded to the results of the biopsies and other clinical data including age and gender, with careful consideration to avoid lesion margins, normal-appearing marrow, endplates, spondylotic changes, and vessels (including the basivertebral venous plexus). Anatomical T_1-weighted precontrast and STIR sequences that matched the DCE-MRI maps were used for optimal ROI placements. For the purpose of normalizing parameters to a ratio of fracture value/normal marrow value, ROIs were also placed in normal marrow of adjacent healthy-looking vertebral bodies avoiding vertebrae with postradiation or abnormal signal changes.

Morphologic Analysis

Two experienced neuroradiologists (J.L. and A.H.) who were not aware of the quantitative DCE data results described the morphological characteristics of the different groups on T_1-weighted precontrast and STIR sequences. These included the T_1 and STIR signal intensity of each fracture and the number of fractures for each patient. Parametric perfusion maps were also visually evaluated for each comparison. Time intensity curves (TIC) were used to compare the pattern of the contrast-uptake in the lesions.

Statistical analysis

A Mann–Whitney U-test at a significance level of corrected $P < 0.01$ was conducted to assess the difference of the DCE-MRI perfusion parameters between pathologic and benign

vertebral fractures. The same test was applied to compare acute and chronic benign fractures, and pathologic and acute fractures. The significance was achieved after a Bonferroni adjustment. In addition, the receiver operating characteristic (ROC) curve analysis was applied to assess the sensitivity and specificity of perfusion parameters between the two pathologies. In the ROC curve analysis, cutoff values determined by maximizing the sum of the sensitivity and specificity were determined for each comparison.

Results

Patients

Patient demographics and fractures classification information for benign (acute and chronic) and pathologic fractures groups is displayed in Tables 1 and 2. There were differences in groups based on age with a mean age of 66 years for the benign group and a mean age for the pathologic group 61.5 years. Most fractures were located in lower thoracic and upper lumbar levels (T11–L3) in both cohorts. Gender distribution was slightly uneven, with most of the pathologic fractures being male (8 of 12) and the benign group having a female predominance (6 of 11).

Conventional MR and Perfusion Maps

Most osteoporotic fractures presented a low-signal-region on T_1-weighted images with areas of spared normal bone. Only the benign group presented with multiple vertebral body fractures. All acute fractures demonstrated varying levels of increased signal on the STIR sequence (Fig. 1). For the subjective analysis, all five parametric perfusion maps demonstrated high signal intensity for all perfusion parameters in the fractured vertebral body, whereas the chronic fractures demonstrated low signal intensity. Pathologic fractures usually exhibited both low signal on T_1-weighted sequences and high signal in STIR sequences. Some cases showed abnormal intensity in different parts of the vertebrae, for example, the pedicle or the paravertebral soft tissues. All perfusion maps in the malignant fracture group depicted increased intensity perfusion values in the fractured vertebral body and sometimes also in other parts of the vertebrae (Fig. 1). Time intensity curves for pathologic fractures showed higher signal intensities for the higher slope threshold curves (Fig. 2).

Quantitative Perfusion Analysis

The mean and standard deviations of the perfusion parameters from the three groups are shown in Fig. 3. Pathologic fractures had significantly higher perfusion parameters (V_p, K^{trans}, wash-in slope, peak enhancement, and AUC) ($P < 0.01$ for each parameter) when compared with benign fractures. We also found significant differences ($P < 0.001$) in all parameters (V_p, K^{trans}, wash-in slope, peak enhancement, and AUC) between chronic benign and acute benign fractures. V_p and K^{trans} were also able to discriminate between pathologic and acute benign fractures ($P < 0.01$). Wash-in was also significant (P=0.02). No significant differences were found with peak enhancement ($P = 0.21$) and AUC ($P = 0.4$) in this last group.

The ROC curve, which depicts the sensitivity and specificity of perfusion parameters for different comparisons, is displayed in Fig. 4. In the first comparison we carried out (pathologic vs. benign fractures), K^{trans} showed the highest AUC (0.902). V_p recorded the second highest AUC (0.876) and was followed by wash-in slope (AUC, 0.857) peak enhancement (AUC, 0.801), and AUC (AUC, 0.773). The second comparison (benign acute vs. chronic fractures) both peak enhancement and AUC demonstrated the highest AUC = 1, followed by K^{trans} (AUC, 0.99), wash-in slope (AUC, 0.969), and V_p (AUC, 0.928). Finally, the third comparison (pathologic vs. acute benign) established K^{trans} as the highest AUC (0.818). It was followed by V_p (AUC, 0.768), wash-in slope (AUC, 0.733) peak enhancement (AUC, 0.628), and AUC (AUC, 0.575). The cutoff values for all perfusion parameters are presented in Table 3.

Discussion

The goal of this study was to evaluate different perfusion parameters and assess differences between benign and malignant vertebral fractures. We performed a quantitative and semiquantitative analysis based on a two-compartment exchange model providing estimates of perfusion and permeability. Our results yielded significant differences between pathologic and osteoporotic fractures, between acute and chronic fractures, and also between acute and pathologic vertebral fractures. Of the five perfusion parameters studied, K^{trans} stands out as the best discriminator between benign osteoporotic versus pathologic vertebral fractures.

All perfusion parameters were notably lower in the chronic fractures compared to acute fractures This is probably due to the sclerotic/fibrotic changes and altered trabecular architecture in the chronically fractured vertebral body, which led to decreased vascularization (V_p) and decreased leakage (K^{trans}). A prior study demonstrated that the age of a fracture notably influences the perfusion parameters.[17] Our findings showed a good agreement with their work, in that perfusion parameters demonstrated significant differences ($P \leq 0.001$) between acute and chronic vertebral fractures.

A number of stages can be distinguished in the fracture healing process: callus proliferation, vascularization, calcification, and reorganization. These stages represent an inflammatory phase, a reparative phase, and a remolding phase.[18] Increased vascularity is observed at the fracture site during the acute inflammatory phase. Therefore, an acute fracture during the inflammatory phase and a pathological fracture can appear similar on DCE, as both will demonstrate increased perfusion characteristics.[10] Notwithstanding, our results showed that K^{trans} and V_p were able to differentiate between acute benign and pathologic fractures. The K^{trans} and V_p values were significantly greater in hotspots in malignant fractures than in benign fractures ($P < 0.01$). A possible explanation for this can be that although the acute inflammatory response to the fracture can show an increase in vascularity and permeability as a part of the healing process, a vertebral body with metastatic deposits will have additional alterations to the microvascular structure. Thus, new fragile vessels in addition to the inflammatory healing changes of the fracture will lead to increased plasma volume as well as augmented vascular permeability.

Discrimination between benign from malignant fractures has been typically based on the evaluation of morphologic parameters such as size, demarcation of margins, involvement of adjacent structures, signal homogeneity, and measurements of relaxation times.[10] Unfortunately, using morphological parameters remains problematic, as there is a substantial overlap between osteoporotic and pathological fractures.

Advanced MRI techniques such as diffusion-weighted MRI have been used in recent years to distinguish pathologic and benign vertebral fractures. Since Baur et al [19] reported that diffusion-weighted imaging (DWI) provided excellent discrimination between pathologic and benign compression fractures, subsequent studies have shown promising results. Sung et al [20] concluded that adding qualitative and quantitative axial DWI to a standard MRI protocol improved the diagnostic accuracy in the differentiation between acute benign and malignant compression fractures of the spine at 3.0T.

Several qualitative and quantitative techniques have been described to evaluate dynamic contrast-enhanced images in spine fractures. In previous studies using semiquantitative analysis of DCE-MRI perfusion parameters, investigators have reported contradictory results regarding the potential of perfusion parameters for the differentiation of benign osteoporotic vertebral fractures from malignant vertebral fractures.[17] Chen et al [4] reported no significant differences in the peak contrast enhancement percentage, enhancement slope, and the time–intensity curve (TIC) patterns between benign acute compression fracture, metastatic vertebral lesion, and pathologic compression fracture. Tokuda et al [10] reported significantly higher peak enhancement, steepest slope, and slope values in pathologic compression fractures than osteoporotic compression fractures, although TIC patterns could not distinguish between the two entities. The results of these previous studies are contradictory regarding the potential of semiquantitative perfusion indexes to distinguish between benign vertebral fractures from malignant vertebral fractures. A great limitation of the former studies is the use of semiquantitative and descriptive parameters, while not taking into account the AIF.[17] In our study most cases demonstrated variable curve patterns, with the most common one depicting a rapidly rising slope (wash-in) during an initial short period followed by a short plateau and a slow wash-out phase. Unlike in the studies by Chen et al and Tokuda et al, no representative pattern of TIC for each group of fractures was found in our study. Instead, we used quantitative and semiquantitative parametric maps taking into account the AIF that, in our view, represents a more reproducible and objective approach.

Geith et al [17] demonstrated that the quantitative perfusion parameters of interstitial volume, ECV, and extraction flow were significantly greater in areas of high plasma flow in acute osteoporotic vertebral fractures compared to acute malignant vertebral fractures. They also observed that the mean values of K^{trans}, plasma flow, and V_p were higher in the areas of increased plasma flow in malignant fractures than in osteoporotic fractures, although no significant differences were detected.[17] Our analysis confirmed their findings that the mean values of DCE-MRI perfusion parameters demonstrated significant differences between benign and pathologic vertebral fractures. Further, we also demonstrated that quantitative DCE-MRI perfusion parameters K^{trans} and V_p are superior to semiquantitative parameters in discriminating acute benign from pathologic vertebral fractures. The ability of our study to obtain significant results, not obtained by Geith et al, may be due to patient selection, as all

of our patients were biopsy-proven, whereas the diagnosis in the Geith et al study was occasionally established by methods outside of histological analysis such as clinical follow up, positron emission tomography, computed tomography (PET-CT), and follow-up with MRI, which may have lead to errors in diagnosis.

There are several possible limitations to our study including a small number of patients and the sampling of only selected regions of the fractures with the ROIs. We followed a standard method of analyzing perfusion data by selecting ROI, which has been shown to be reproducible, although it remains a subjective operator-dependent technique, associating an inevitable factor of interobserver and intraobserver variability. In spite of the fact that we recruited consecutive patients that met the inclusion criteria, this is a retrospective study and there is a possibility of selection bias. No stratification according to primary malignancies was made within the malignant fracture group, although there might be different perfusion patterns of the metastatic deposits responsible for the fractures, expecting high perfusion parameters in metastasis from hypervascular tumors and vice versa.[21] This study has a wide range of patient age (46–84 years old) and some authors have reported that dynamic contrast enhancement of bone marrow can be strongly influenced by age and fat content.[10] However, the patients in this study were all middle age or older adults, hence minimizing age-related variations. Even though the influence of fat content was not taken into account during perfusion analyses, it should be negligible because the fat fraction is known to be very small in fractures.[17] Few of the patients in this study had benign osteoporotic fractures, as most patients with osteoporotic fractures could be diagnosed using conventional imaging and thus avoided biopsy. The patients with benign fractures who were included in this study had undergone biopsy as part of a kyphoplasty procedure. Also, we analyzed multiple compression fractures from a single patient as independent lesions with the assumption that underlying systemic patient-related factors would not bias these results.

Our data demonstrate that quantitative evaluation of DCE-MRI can be used as a noninvasive analytical indicator to distinguish between pathologic and benign, acute and chronic, and most important, benign acute and pathologic vertebral fractures. The value of DCE-MRI in differentiating the nature of fractures has potential clinical implications. Adding DCE perfusion maps to standard MRI may improve diagnostic accuracy and may significantly impact patient care outcomes.

Acknowledgments

This article was accepted as an oral presentation at the 2014 RSNA Meeting.

Contract grant sponsor: Spanish Foundation Fundación Alfonso Martín Escudero (to J.A.-P.).

The grant name is “NIH/NCI Cancer Center Support Grant P30 CA008748.”

References

1. Jung HS, Jee WH, McCauley TR, Ha KY, Choi KH. Discrimination of metastatic from acute osteoporotic compression spinal fractures with MR imaging. Radiographics. 2003; 23:179–187. [PubMed: 12533652]
2. Croarkin E. Osteopenia in the patient with cancer. Phys Ther. 1999; 79:196–201. [PubMed: 10029059]

3. Gold RI, Seeger LL, Bassett LW, Steckel RJ. An integrated approach to the evaluation of metastatic bone disease. Radiol Clin North Am. 1990; 28:471–483. [PubMed: 2408106]
4. Chen WT, Shih TT, Chen RC, et al. Blood perfusion of vertebral lesions evaluated with gadolinium-enhanced dynamic MRI: in comparison with compression fracture and metastasis. J Magn Reson Imaging. 2002; 15:308–314. [PubMed: 11891976]
5. Jacobsson H, Goransson H. Radiological detection of bone and bone marrow metastases. Med Oncol Tumor Pharmacother. 1991; 8:253– 260. [PubMed: 1820491]
6. Yamaguchi T, Tamai K, Yamato M, Honma K, Ueda Y, Saotome K. Intertrabecular pattern of tumors metastatic to bone. Cancer. 1996; 78:1388–1394. [PubMed: 8839543]
7. Biffar A, Sourbron S, Dietrich O, et al. Combined diffusion-weighted and dynamic contrast-enhanced imaging of patients with acute osteoporotic vertebral fractures. Eur J Radiol. 2010; 76:298–303. [PubMed: 20580503]
8. Verstraete KL, Van der Woude HJ, Hogendoorn PC, De-Deene Y, Kunnen M, Bloem JL. Dynamic contrast-enhanced MR imaging of musculoskeletal tumors: basic principles and clinical applications. J Magn Reson Imaging. 1996; 6:311–321. [PubMed: 9132096]
9. Roodman GD. Mechanisms of bone lesions in multiple myeloma and lymphoma. Cancer. 1997; 80(8 Suppl):1557–1563. [PubMed: 9362422]
10. Tokuda O, Hayashi N, Taguchi K, Matsunaga N. Dynamic contrast-enhanced perfusion MR imaging of diseased vertebrae: analysis of three parameters and the distribution of the time-intensity curve patterns. Skeletal Radiol. 2005; 34:632–638. [PubMed: 16091963]
11. Tofts PS, Brix G, Buckley DL, et al. Estimating kinetic parameters from dynamic contrast-enhanced T(1)-weighted MRI of a diffusable tracer: standardized quantities and symbols. J Magn Reson Imaging. 1999; 10:223–232. [PubMed: 10508281]
12. Chu S, Karimi S, Peck KK, et al. Measurement of blood perfusion in spinal metastases with dynamic contrast-enhanced magnetic resonance imaging: evaluation of tumor response to radiation therapy. Spine. 2013; 38:E1418–1424. [PubMed: 23873238]
13. van der Woude HJ, Verstraete KL, Hogendoorn PC, Taminiau AH, Hermans J, Bloem JL. Musculoskeletal tumors: does fast dynamic contrast-enhanced subtraction MR imaging contribute to the characterization? Radiology. 1998; 208:821–828. [PubMed: 9722866]
14. Moulopoulos LA, Maris TG, Papanikolaou N, Panagi G, Vlahos L, Dimopoulos MA. Detection of malignant bone marrow involvement with dynamic contrast-enhanced magnetic resonance imaging. Ann Oncol. 2003; 14:152–158. [PubMed: 12488307]
15. Hawighorst H, Libicher M, Knopp MV, Moehler T, Kauffmann GW, Kaick G. Evaluation of angiogenesis and perfusion of bone marrow lesions: role of semiquantitative and quantitative dynamic MRI. J Magn Reson Imaging. 1999; 10:286–294. [PubMed: 10508288]
16. Stabler A, Baur A, Bartl R, Munker R, Lamerz R, Reiser MF. Contrast enhancement and quantitative signal analysis in MR imaging of multiple myeloma: assessment of focal and diffuse growth patterns in marrow correlated with biopsies and survival rates. AJR Am J Roentgenol. 1996; 167:1029–1036. [PubMed: 8819407]
17. Geith T, Biffar A, Schmidt G, et al. Quantitative analysis of acute benign and malignant vertebral body fractures using dynamic contrast-enhanced MRI. AJR Am J Roentgenol. 2013; 200:W635–643. [PubMed: 23701095]
18. Cruses, RL., Dumont, J. Healing of bone, tendon and ligament. In: Rockwood, CA., Jr, Green, DP., editors. Fractures. Philadelphia: JB Lippincott; 1975. p. 97-98.
19. Baur A, Stabler A, Bruning R, et al. Diffusion-weighted MR imaging of bone marrow: differentiation of benign versus pathologic compression fractures. Radiology. 1998; 207:349–356. [PubMed: 9577479]
20. Sung JK, Jee WH, Jung JY, et al. Differentiation of acute osteoporotic and malignant compression fractures of the spine: use of additive qualitative and quantitative axial diffusion-weighted MR imaging to conventional MR imaging at 3.0 T. Radiology. 2014; 271:488–498. [PubMed: 24484060]
21. Khadem NR, Karimi S, Peck KK, et al. Characterizing hypervascular and hypovascular metastases and normal bone marrow of the spine using dynamic contrast-enhanced MR imaging. AJNR Am J Neuroradiol. 2012; 33:2178–2185. [PubMed: 22555585]

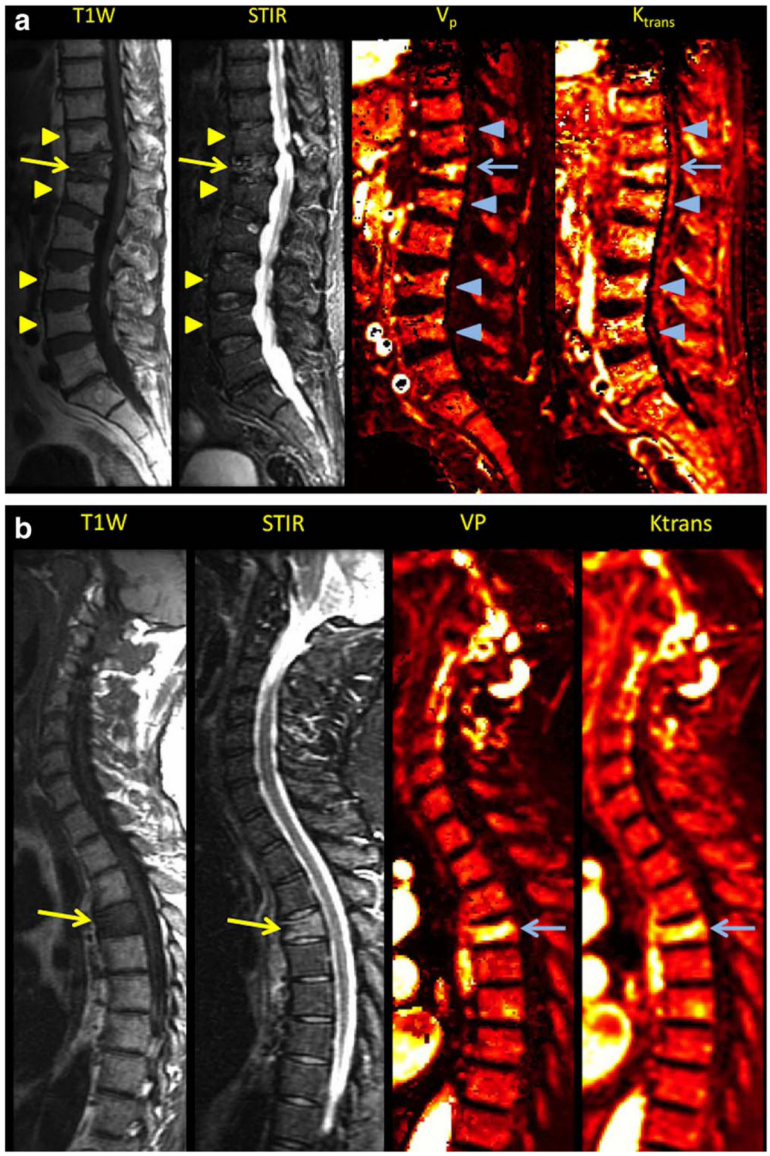

FIGURE 1.

A: Sagittal T_1-weighted, STIR MR images matching with corresponding V_p and K^{trans} maps depicting simultaneously chronic benign vertebral fractures (arrowheads) and acute benign vertebral fracture (arrow). Signal intensity changes and increased V_p and K^{trans} values are noted in the acute vertebral fracture in conventional sequences and parametric maps, respectively. B: Sagittal T_1-weighted, STIR MR images paired with corresponding V_p and K^{trans} maps depicting pathologic vertebral fractures (arrows). Signal intensity changes and increased V_p and K^{trans} values are noted in the conventional sequences and parametric maps, respectively.

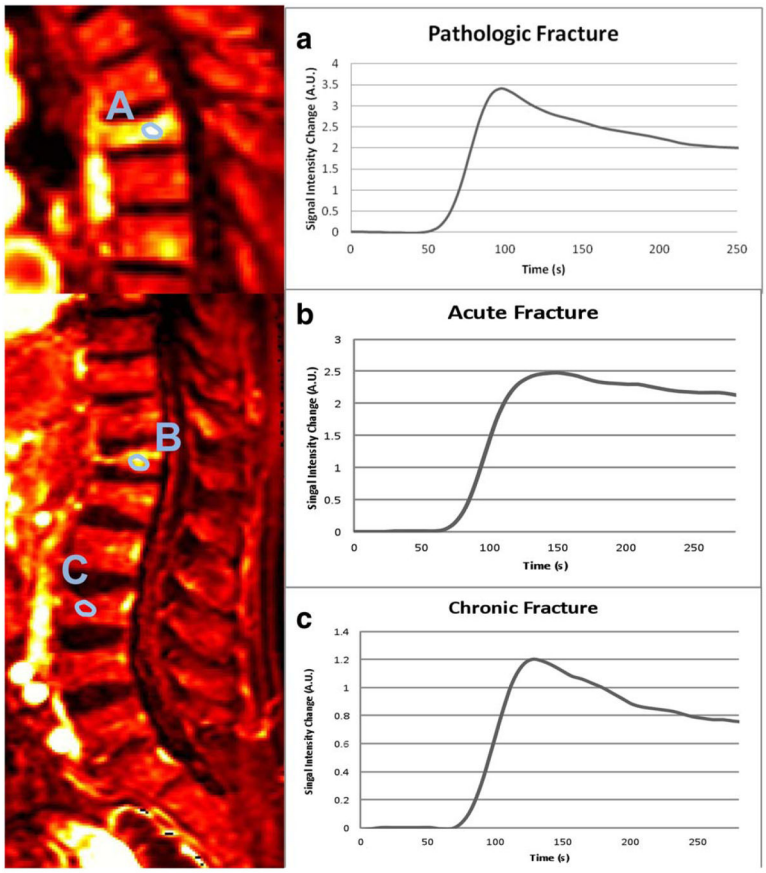

FIGURE 2.

Sagittal perfusion maps (K^{trans}) from a patient with a pathologic fracture (**A**) and another patient presenting acute (**B**) and chronic benign (**C**) fractures simultaneously paired with corresponding time–intensity curves.

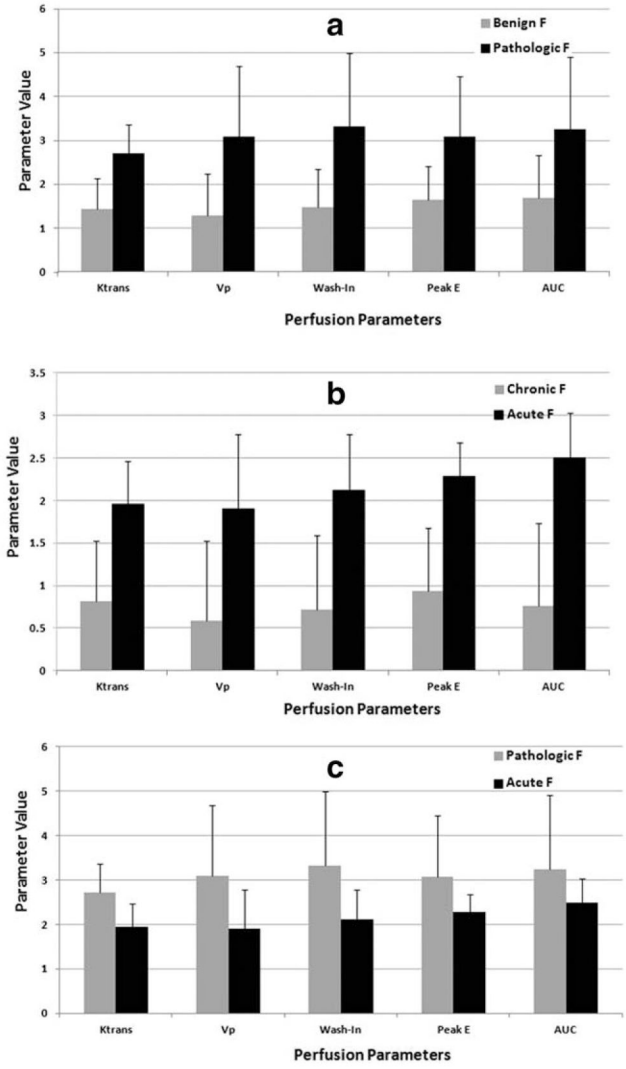

FIGURE 3.

A bar graph illustrating the mean values and standard deviations for the DCE-MRI perfusion parameters K^{trans}, V_p, wash-in, and peak-enhancement in pathologic vs. benign fractures (**A**), benign acute vs. chronic (**B**), and acute vs. pathologic (**C**).

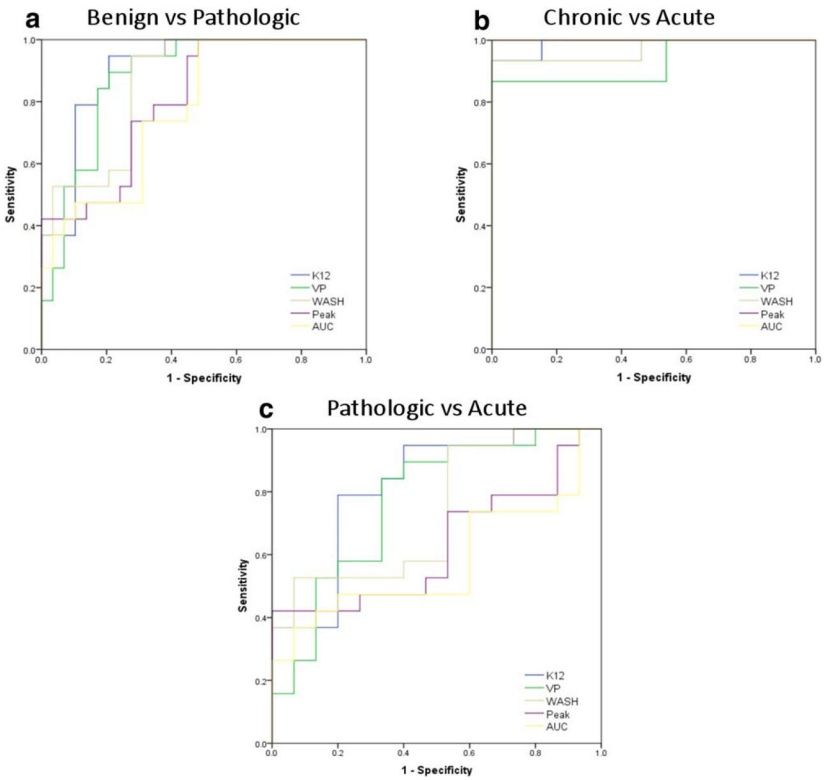

FIGURE 4.

ROC curves depicting the true-positive rate (specificity) and the false-positive rate (sensitivity) of DCE-MRI perfusion parameters in classifying benign vs. pathologic fractures (**A**), chronic vs. acute fractures (**B**), and pathologic vs. acute (**C**).

TABLE 1

Demographics

		Total	Nonpathologic		Pathologic
			Chronic	Acute	
Patients (*n*)		21	4[a]	7[a]	12
Fractures (*n*, %)		47	13 (27.66%)	15 (31.91%)	19 (40.43%)
Gender (*n*)	Female	9	3	3	4
	Male	12	1	4	8

[a]Acute and chronic fractures were present simultaneously in two patients.

TABLE 2

Demographics for Patients With Vertebral Fractures

Patient	Age	Gender	Level of fracture	Biopsy/concomitant malignancy
Pathologic Fractures				
1	76	M	L1	Lung adenocarcinoma
2	56	M	L4	Colon adenocarcinoma
3	78	M	L5	Colon adenocarcinoma
4	58	M	T4	Gastric adenocarcinoma
5	56	M	L1	Melanoma
6	66	M	T12	Renal cell carcinoma
7	46	M	T12	Gastric adenocarcinoma
8	51	F	L2	Colon adenocarcinoma
9	63	F	T11, T12	Lung adenocarcinoma
10	52	F	L2, L3, L5	Lung adenocarcinoma
11	77	M	T8, L2, L3	Prostate adenocarcinoma
12	56	F	T12, L1, L2	Breast adenocarcinoma
Chronic fractures				
1	70	F	L1, L2, L3, L4, L5	Ovarian adenocarcinoma
2	55	M	T11, L1, L3, L4	Multiple myeloma
3	67	F	T12, L1	Sarcoma
4	64	F	L1, L4	Glioblastoma
Acute fractures				
1	68	F	T10,T11, T12	Gallbladder adenocarcinoma
2	71	M	L2, L2, T12	Glioblastoma
3	84	F	T10,T12	Esophageal adenocarcinoma
4	55	M	T12	Multiple myeloma
5	62	M	T9,T11, T12, L1	Glioblastoma
6	62	M	T12	Glioblastoma
7	64	F	T9	Glioblastoma

TABLE 3

Cutoff Values

	Pathologic vs. benign	Acute vs. chronic	Acute vs. pathologic
K^{trans}	1.998 (90%, 79%)	1.27 (93%, 100%)	2.19 (79%, 73%)
V_p	1.91 (89.5%, 79%)	1.25 (87%, 100%)	2.01 (84%, 68%)
Wash-in	1.95 (90%, 71%)	1.198 (93%, 100%)	2.54 (58%, 60%)
Peak	2.09 (79%, 64%)	1.29 (100%, 100%)	2.59 (50%, 73%)
AUC	2 (79%, 54%)	1.29 (100%, 100%)	2.76 (50%, 80%)

Cutoff value (sensitivity, specificity).